Research Article

Study of a Nanocomposite Based on a Conducting Polymer: Polyaniline

Nicolas Kohut-Svelko, Stphanie Reynaud, Rmi Dedryvre,
Herv Martinez, Danielle Gonbeau, and Jeanne Franois

Langmuir, **2005**, 21 (4), 1575-1583• DOI: 10.1021/la0481243 • Publication Date (Web): 15 January 2005

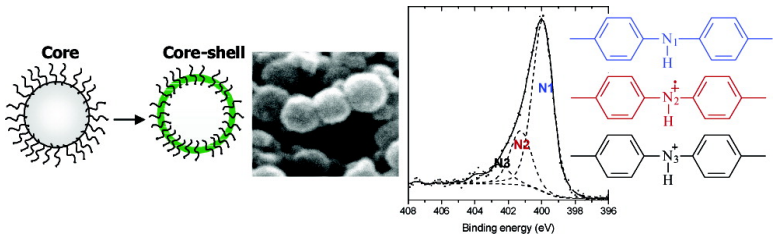

More About This Article

Additional resources and features associated with this article are available within the HTML version:

- Supporting Information
- Links to the 6 articles that cite this article, as of the time of this article download
- Access to high resolution figures
- Links to articles and content related to this article
- Copyright permission to reproduce figures and/or text from this article

View the Full Text HTML

Study of a Nanocomposite Based on a Conducting Polymer: Polyaniline

Nicolas Kohut-Svelko,† Stéphanie Reynaud,*,† Rémi Dedryvère,‡ Hervé Martinez,‡ Danielle Gonbeau,‡ and Jeanne François†

LPCP-UMR 5067 and LCTPCM-UMR 5624, Hélioparc, 2 avenue du président Angot, 64053 Pau Cedex 9, France

Received July 26, 2004. In Final Form: November 2, 2004

A simple way to obtain a conducting nanocomposite is described, and the conducting particles are characterized. Core−shell particles [polystyrene−polyaniline (PANI)] have been obtained by the dispersion process from three types of polystyrene latexes: a no-cross-linked core stabilized by a nonylphenolethoxylate (NP40) and two cross-linked cores stabilized by NP40 and a mixture NP40/Surfamid (a surfactant bearing an amide group). The surface of these particles has been extensively characterized by X-ray photoelectron spectroscopy (XPS), atomic force microscopy, and scanning electron microscopy. A maximum coverage of 94% was obtained for the high PANI content as revealed by XPS analysis. A better coverage was obtained for the cross-linked polystyrene latex stabilized by the Surfamid. The amide group of this surfactant allows the H-bonding formation with the PANI backbone and, thus, improves the conductivity. It was shown that a uniform coverage of the core particles was not required to ensure a good conductivity.

Introduction

Since the discovery of intrinsically conducting polymers (ICPs), the scientific community has interest in understanding and finding applications of such materials. The most common ICPs are polyacetylene, polythiophene, polypyrrole (PPy), and polyaniline (PANI). Conducting polymers have the electronic properties of a semiconductor as well as the mechanical properties of polymers. Nevertheless, these polymers are difficult to process as a result of their insolubility in common solvents and their infusibility. To overcome this drawback, significant progress have been made in the processing of ICPs. Among conducting polymers, PANI remains the most attractive because it is stable under ambient conditions. To improve its processability, the synthesis of the PANI in colloidal form has been described. The first method consists of polymerizing the monomer (aniline) in the presence of a water-soluble surfactant. Such a colloid can be obtained by using a wide range of commercial water-soluble polymers known for their ability to stabilize an emulsion, poly(vinyl alcohol),[1] poly(vinyl pyrrolidone),[2] or handmade stabilizers. More recently, a second method has been proposed using a core−shell-like structure. The core constituted by inorganic polymer[3−5] or vinylpolymer[6−8] gives to the system mechanical properties while a conducting polymer lying in the shell provides its conductivity. In such systems, it has been demonstrated that the resulting conductivity depends on many parameters: the nature of the core composition,[9,10] the surfactant,[11,12] and the method of synthesis of the conducting polymer.[6,13] In fact, we can expect that these parameters play an important role on the structure of the conducting polymer shell and consequently on the conductivity. Generally, commercial latexes have been used as precursors and poor conductivity of the resulting composites has been obtained. Moreover, the PANI deposition onto submicrometer-sized latexes was less uniform compared to that for micrometer-sized latex, and this system remains to be optimized.

Our group focused on the optimization of a simple route to yield to a conductive nanocomposite in one step following the core−shell strategy. The core as well as the core−shell particles were synthesized to control all the steps of the process and the composition of the dispersion. Commercially available products are used in soft experimental conditions, that is, without external acid or organic solvent. Three seed latexes were synthesized by changing the surfactant nature. First, a nonylphenolethoxylate (NP40) with 40 units of ethoxylate was used. NP40 does not interact with the PANI. Second, a mixture of NP40 and a surfactant bearing an amide group (Surfamid) was used. This kind of structure allows the formation of hydrogen bonds with a PANI backbone and is expected to improve the conductivity of the resulting composite. The conductive composite is obtained at the end of the process and needs no post-treatment.

X-ray photoelectron spectroscopy (XPS) is known to be a powerful method to investigate and characterize the core−shell particles and provides information about chemical composition on the extreme surface (depth ca.

* To whom correspondence should be addressed. E-mail: stephanie.reynaud@univ-pau.fr.

† LPCP-UMR 5067.

‡ LCTPCM-UMR 5624.

(1) Stejskal, J.; Kratochvil, P.; Gospodinova, N.; Terlemezyan, L.; Mokreva, P. *Polymer* **1992**, *33*, 4857.

(2) Ghosh, P.; Siddhanta, S. K.; Chakrabarti, A. *Eur. Polym. J.* **1999**, *35*, 699.

(3) Han, M. G.; Armes, S. P. *J. Colloid Interface Sci.* **2003**, *262*, 418.

(4) Gill, M.; Armes, S. P.; Fairhurst, D.; Emmett, S. N.; Idzorek, G.; Pigott, T. *Langmuir* **1992**, *8*, 2178.

(5) Han, M. G.; Armes, S. P. *Langmuir* **2003**, *19*, 4523.

(6) Barthet, C.; Armes, S. P.; Lascelles, S. F.; Luk, S. Y.; Stanley, H. M. E. *Langmuir* **1998**, *14*, 2032.

(7) Cairns, D. B.; Armes, S. P.; Bremer, L. G. B. *Langmuir* **1999**, *15*, 8052.

(8) Khan, M. A.; Armes, S. P. *Langmuir* **1999**, *15*, 3469.

(9) Perruchot, C.; Chehimi, M. M.; Delamar, M.; Lascelles, S. F.; Armes, S. P. *Langmuir* **1996**, *12*, 3245.

(10) Maeda, S.; Gill, M.; Armes, S. P.; Fletcher, I. W. *Langmuir* **1995**, *11*, 1899.

(11) Khan, M. A.; Armes, S. P.; Perruchot, C.; Ouamara, H.; Chehimi, M. M.; Greaves, S. J.; Watts, J. F. *Langmuir* **2000**, *16*, 4171.

(12) Cairns, D. B.; Armes, S. P.; Chehimi, M. M.; Perruchot, C.; Delamar, M. *Langmuir* **1999**, *15*, 8059.

(13) Barthet, C.; Armes, S. P.; Chehimi, M. M.; Bilem, C.; Omastova, M. *Langmuir* **1998**, *14*, 5032.

10.1021/la0481243 CCC: $30.25
Published on Web 01/15/2005

5 nm).[9−14] Many studies were carried out to characterize conducting organic polymers such as PPy,[9,12] PANI,[13] or poly(3,4-ethylenedioxythiophene) (PEDOT).[11]

On the other hand, atomic force microscopy (AFM) has attracted most attention for the study of such polymeric materials because both conducting and nonconducting samples can be imaged, which is not the case by conventional scanning electron microscopy (SEM) analysis. In addition, AFM has been used to study the size distribution and structural organization of uncoated and coated latex particles.[15−17]

In the present paper, we focused on the study of the PANI coverage onto submicrometer-sized polystyrene (PS) latex particles. The synthesis was optimized to give a conductive composite in soft conditions. The aim of this study was to connect the chemical structure (characterized by XPS, SEM, and AFM) and the conductivity of the composite.

Experimental Section

Materials. Styrene was received from Aldrich and was purified by passing through a basic activated alumina column before use. Igepal CO 897 (called NP40, hydrophilic−lypophilic balance = 17.8) was obtained from Rhodia. The surfactant bearing an amide group (called Surfamid) was obtained from Stepan. This surfactant is a lauramideethoxylate with six units of ethoxylate. The surfactants were used as received. Ammonium persulfate [APS, $(NH_4)_2S_2O_8$], aniline hydrochloride, and divinylbenzene were obtained from Aldrich and used as received. Water was distilled before use. All other products were used as received unless otherwise noted.

HCl-Doped PANI. Conventional HCl-doped PANI was synthesized following the classical method.[18] An aqueous solution of APS (0.0504 mol in 200 mL of 1 M HCl) was added to an aniline solution (0.219 mol in 300 mL of 1 M HCl) at 1 °C. Polymerization was carried out at 0 °C for 5 h.

Core−Shell Synthesis. The core particles were synthesized according to the procedure described by El-Aasser et al.[19] The reaction vessel was purged with nitrogen to remove all traces of oxygen. In a typical polymerization, surfactant (3.34 g) was dissolved under a nitrogen atmosphere in distilled water (200 mL) in a three-necked round-bottom flask. The purified monomer (styrene, 87 g, 0.836 mol) was added to the aqueous solution and emulsified under vigorous stirring. This emulsion was then heated under mechanical stirring up to 70 °C. The aqueous solution of APS (0.3 g in 5 mL of water) was then added drop by drop. The polymerization was then allowed to process for 24 h at 70 °C under mechanical stirring.

Samples of the final core latex particles were made and purified by four centrifugation/redispersion cycles (20 000 rotations/min, 5 °C, 30 min) by replacing the supernatant by fresh distilled water. At the last centrifugation, the supernatant is colorless.

In a second stage, aniline hydrochloride is used as the monomer and is added to the above dispersion of PS to create a core−shell structure. The concentration of aniline hydrochloride was kept constant (15 mg/mL), and the solid content of the PS latex is adjusted with the respect to the expected core−shell ratio. Neither additional acid nor surfactant was added to the reaction mixture. The core dispersion containing the aniline hydrochloride was left under stirring for 20 min before being cooled to 0 °C for 1 h.

The oxidant solution (APS in water) was then added drop by drop to the above dispersion ([oxidant]/[aniline hydrochloride] = 1). Polymerization is carried out under nitrogen and magnetic stirring; the temperature is maintained at 0 °C for 5 h. The reaction mixture was then left at room temperature under stirring for 19 h.[6] The sample of the dark final dispersion was purified by repeated centrifugation−redispersion cycles; the successive supernatants were replaced by distilled water to remove the residual initiator and monomer.

Cross-Linked Core Latexes. For the synthesis of the cross-linked core, a procedure the same as that described above was used. The divinylbenzene (3−4 wt % vs styrene) was used as the cross-link agent and was added at the same time as the monomer.

Characterization Techniques. *Conductivity Measurements.* The conductivity of compressed pellets (under 5 ton/cm^2) of the composite was determined using the standard four-point probe technique at room temperature with an home-built device. Three pellets of each composite were prepared, and then 36 measurements were made: six on each side of the pellets. The reproducibility is 1 ± 0.15 S/cm.

Dynamic Light scattering (DLS). The particles size was measured on a DL 135-45, DLS apparatus developed by the IFP (French Petroleum Institute). The technique works on a very thin suspension layer to avoid multiscattering phenomena and can be successfully applied to concentrated, dense, and opaque solutions. It is equipped with a laser (wavelength 633 nm).

The results were confirmed by classical DLS (Sematech) on very diluted latex solutions (solvent, water; wavelength, 514.5 nm).

XPS. XPS measurements were carried out with a Kratos Axis Ultra spectrometer, using a focused monochromatic Al Kα radiation (1486.6 eV). Core peaks and valence band spectra were recorded with a 20-eV constant pass energy. The analyzed area of the samples was 300 × 700 μm^2 so that samples can be considered to be homogeneous in the analysis area. Charge neutralization was used for all measurements, the pressure in the analysis chamber was about 5×10^{-7} Pa, and the temperature of the samples was regulated at −134 °C to avoid a possible degradation due to the X-ray beam. Short-time spectra were recorded at the beginning and at the end of each experiment to check the nondegradation of the samples. The binding energy scale was calibrated from the C(1s) peak of PS at 284.8 eV. Core peaks were analyzed using a nonlinear Shirley-type background,[20] and peak positions and areas were obtained by a weighted least-squares fitting of model curves (70% Gaussian, 30% Lorentzian) to the experimental data.

AFM. The samples were imaged under ambient conditions using a commercial (CP from Park Scientific Instrument) AFM head, controlled by feedback electronics and software of conventional design. In this study, AFM with a laser beam deflection sensor is applied. Cantilever-type Si_3N_4 springs with integrated tips are used as force sensors. Typical tip radii of curvature are 20 nm, and the spring constant is 0.07 N/m. Images were recorded in the constant force mode, in the range 10−20 nN with a low scan frequency (0.5 Hz). The 1-μm grill and mica used as calibration samples always gave the correct periodicity. All images are displayed in the gray scale such that the dark region corresponds to areas of lower height than the light regions.

SEM. Morphology studies were carried out using an environmental scanning electron microscope ElectroScan instrument operating at 20 kV. The samples were mounted on a double-sided adhesive carbon disks, and no gold coating is needed.

NMR. ^{1}H NMR spectra of the surfactant were recorded at 400 MHz on a Bruker Advanced AM400 spectrometer in $CDCl_3$, and the chemical shifts in ppm are referred to the internal standard: tetramethylsilane.

Results and Discussion

Seed latexes. Three kinds of seed latexes have been synthesized. The first kind is a seed PS latex stabilized by the surfactant NP40 and called PS(NP40). DLS measurements and SEM analysis have shown that the

(14) Briggs, D.; Seah, M. P. In *Practical Surface Analysis by Auger and X-ray Photoelectron Spectroscopy*; Briggs, D., Ed.; J. Wiley and Sons: New York, 1983.
(15) Meincken, M.; Sanderson, R. D. *Polymer* **2002**, *43*, 4947.
(16) Zhang, P.-C.; Liu, J.; Chew, C. H.; Gan, L. M.; Li, S. F. Y. *Talanta* **1998**, *45*, 767.
(17) Laranjeira, J. M. G.; da Silva, J. E. F.; de Azevedo, W. M.; de Vasconcelos, E. A.; Khoury, H. J.; Simao, R. A.; Achete, C. A. *Microelectron. J.* **2003**, *34*, 511.
(18) MacDiarmid, A. G.; Chiang, J. C.; Richter, A. F.; Somasiri, N. L. D.; Epstein, A. J. In *Conducting Polymers*; Alcacer, L., Ed.; D. Reidel Publishing Company: Dortrecht, The Netherlands, 1987.
(19) Ozdeger, E.; Sudol, E. D.; El-Aasser, M. S.; Klein, A. *J. Polym. Sci., Part A: Polym. Chem.* **1997**, *35*, 3813.
(20) Scofield, J. H. *J. Electron Spectrosc.* **1976**, *8*, 129.

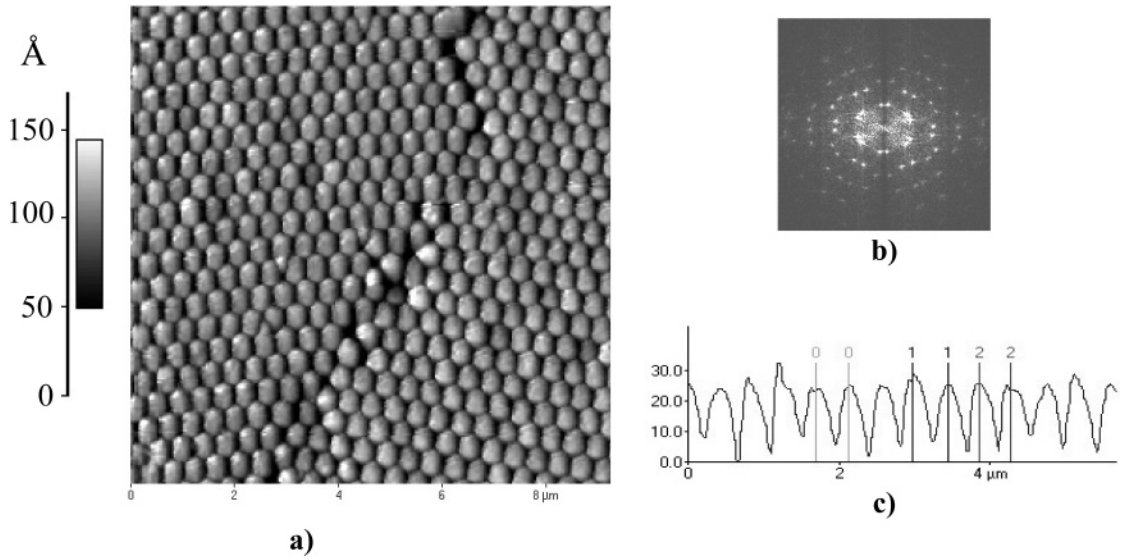

Figure 1. (a) AFM images of PS-CL latex particles, (b) FT spectrum, and (c) height profile.

particles exhibited a bimodal distribution: 60% by number of particles with a diameter of 360 nm and 40% with a diameter of 140 nm. This feature has been attributed to the method of synthesis and the occurrence of a second nucleation as detailed by other authors.[21,22]

The second kind was a cross-linked PS latex stabilized by NP40. This PS-CL(NP40) was characterized by AFM as shown in Figure 1. It exhibits a regular one-dimensional linear ordered arrangement (confirmed by the diffraction pattern obtained by Fourier transform, Figure 1b, and a narrow size distribution. Note that the AFM image does not clearly exhibit spherical particles as it is expected. This feature could be explained by the contact mode of operation (which involves friction forces), even if the lowest force as possible was applied to the cantilever in contact with the surface of the material. Nevertheless, the latex particles are organized in a close-packed structure and their size was measured by the height profile along a direction as shown in Figure 1c. The peak-to-peak distance was an average of several height profiles in several directions to minimize the preferential deformation along one direction. The peak-to-peak distance was measured in the range of 350−370 nm, which is in good agreement with the results obtained by light scattering (mean diameter, $D = 360$ nm). The low value (6 Å) of the root-mean-squared (rms) roughness is also indicative of a uniform distribution of the latex particles on the surface.

The third kind was a cross-linked PS latex stabilized by a mixture of NP40 and Surfamid, called PS-CL(NP40/Surfamid). Particles showed a mean diameter of 340 nm and a monodisperse distribution as measured by DLS. Then, the two cross-linked PS latexes differ only by the nature of the stabilizer.

XPS survey spectra of the seed latexes showed the presence of C and O elements at the surface. All the seed latexes, PS(NP40), PS-CL(NP40), and PS-CL(NP40/Surfamid) exhibit very similar C(1s) core peaks. Therefore, only the C(1s) spectrum of PS(NP40) is shown in Figure 2. The spectrum displays a main peak at 284.8 eV that can be assigned to carbon atoms bound to carbon or hydrogen atoms only. The shoulder observed at 286.6 eV can be assigned to carbon atoms bound to one oxygen in

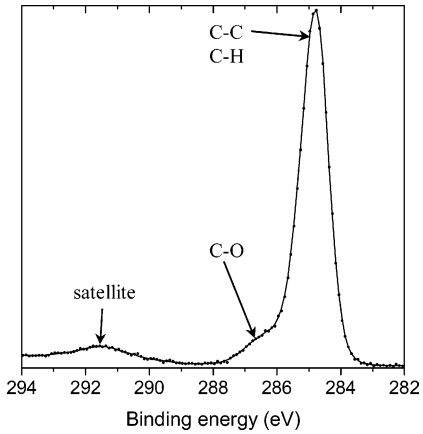

Figure 2. XPS C(1s) spectrum of uncoated PS latex PS(NP40).

the surfactant.[23] Its intensity is in good agreement with the amount of surfactant as measured by ^{1}H NMR (5.4 wt %). The additional peak at 291.5 eV ("shake-up" satellite) can be attributed to multielectronic transitions involving $\pi-\pi^*$ transitions due to the aromatic rings.[14]

PANI Reference: HCl-Doped PANI. The PANI reference synthesis is detailed in the experimental section. XPS survey spectra of this pure doped PANI synthesized by the standard method and called HCl-doped PANI showed the presence of C, O, N, Cl, and S elements. The extremely low Cl/N ratio was already observed by other groups for PANI[13] and PPy[12] polymers. The dopant deficiency could be due to the surface oxidation or to the purification method. The presence of the S element in small quantities is due to the synthesis method. The presence of oxygen is attributed to the oxidant and to extra contaminating oxygen.

Figure 3 shows the N(1s) and C(1s) core spectra of PANI. The N(1s) spectrum displays an asymmetrical profile and can be fitted to three components at 400.0, 401.2, and 402.6 eV. According to previous studies,[24−29]

(21) Piirma, I.; Maw, T. S. *Polym. Bull.* **1984**, *11*, 497.
(22) Piirma, I.; Chang, M. *J. Polym. Sci., Part A: Polym. Chem.* **1982**, *20*, 489.
(23) Zhang, F.; Kang, E. T.; Neoh, K. G.; Wang, P.; Tan, K. L. *Biomaterials* **2002**, *23*, 787.
(24) Kumar, S. N.; Bouyssoux, G.; Gaillard, F. *Surf. Interface Anal.* **1990**, *15*, 531.
(25) Han, M. G.; Im, S. S. *Polymer* **2000**, *41*, 3253.
(26) Chen, Y.; Kang, E. T.; Neoh, K. G.; Wang, P.; Tan, K. L. *Synth. Met.* **2000**, *110*, 47.
(27) Yue, J.; Epstein, A. J. *Macromolecules* **1991**, *24*, 4441.

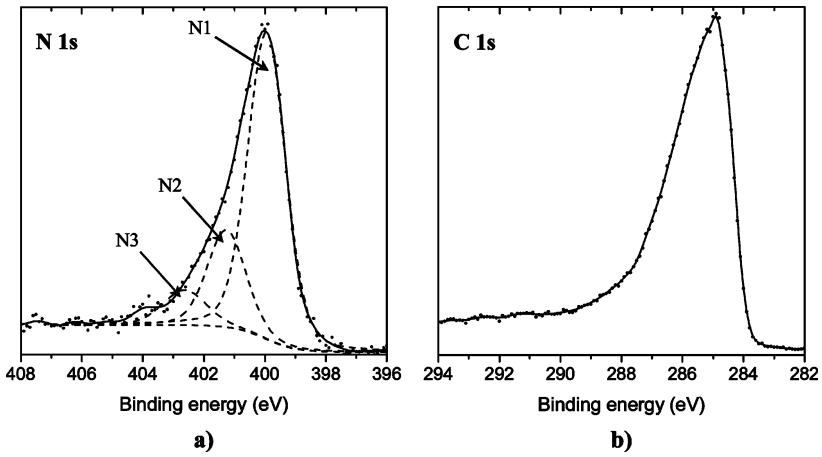

Figure 3. XPS spectra (a) N(1s) and (b) C(1s) of HCl-doped PANI.

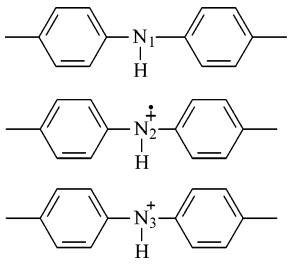

Figure 4. Different kinds of nitrogen in PANI.

these components have been assigned to three kinds of nitrogen[30−35] as shown in Figure 4. The component observed at 400.0 eV is attributed to neutral amine nitrogen atoms (N1), in good agreement with the reference leucoemeraldine (fully reduced PANI) which displays a symmetrical peak at 399.9 eV.[36] The component at 401.2 eV is attributed to nitrogen atoms with a delocalized positive charge $N^{\bullet+}$ (N2), and that observed at 402.6 eV is attributed to the most positively charged nitrogen atoms N^+ (N3). All these peaks are characteristic to the doped PANI (called emeraldine salt). Actually, there is no distinct limit between different kinds of nitrogen because the positive charges are delocalized over the aromatic rings and the whole polymeric chain.

The C(1s) spectrum also displays an asymmetrical profile, as shown in Figure 3b. No fitting has been reported in the figure because no clear assignment can be done for each component. This spectrum is again very different from that of leucoemeraldine, which contains only neutral amine nitrogen atoms (N1) and is an electrical insulator. The C(1s) spectrum of leucoemeraldine (not shown here) displays two distinct narrow peaks, the first at 284.7 eV attributed to C atoms bound only to C or H atoms and the second at 285.9 eV attributed to C atoms bound to one nitrogen.[36] On the contrary, the C(1s) spectrum of HCl-doped PANI, shown in Figure 3b, exhibits a very broad and asymmetrical shape. The different environments of C atoms contribute to this particular shape, but the very important broadening can only be explained by the delocalization of the positive charges over the aromatic cycles, leading to an increase of the density of positive charges on the carbon atoms and resulting in positive chemical shifts.[37]

PS−PANI Composites. From the three kinds of seed latexes, various types of PS−PANI nanocomposites were prepared. A first series was obtained from PS(NP40) by varying the PS/PANI weight ratio: PS(NP40)−PANI (80/20), PS(NP40)−PANI (65/35), and PS(NP40)−PANI (47/53). A second series was prepared by keeping constant the PS/PANI weight ratio (80/20) and varying the nature of the seed latexes. The following composites have been prepared: PS-CL(NP40)−PANI (80/20) and PS-CL(NP40/Surfamid)−PANI (80/20), to investigate the influence of the nature of the seed particles. The experimental core/shell ratios of PS/PANI were obtained by thermogravimetric analysis and UV characterization. A good correlation between the theoretical and the experimental mass loading was found.

All the composites and reference materials have been characterized by XPS to analyze the PANI coverage and the influence of surfactant and core nature.

XPS survey spectra of PS−PANI composites showed the presence of C, N, O, Cl, and S elements at the surface. The presence of Cl and S elements in small quantities is due to the synthesis method. The unexpected low Cl/N ratio is again observed and related to the characterization and synthesis methods as described previously for the HCl-doped PANI. The presence of oxygen is mainly attributed not only to the surfactant NP40 but also to extra contaminating oxygen. C(1s), N(1s), O(1s), Cl(2p), and S(2p) core peaks were recorded, and the corresponding results of quantitative analysis are reported in Table 1. Figure 5 shows C(1s) and N(1s) spectra of seed latex PS-(NP40) (a), PS(NP40)−PANI composites with the core−shell weight ratios 80/20 (b), 65/35 (c), and 47/53 (d), and HCl-doped PANI (e). From a qualitative point of view, we can see in Figure 5-1 a progressive broadening of the C(1s) spectrum when the PANI weight ratio increases. For the highest PANI weight ratio (47/53), a very important broadening and the disappearance of the satellite peak can be observed, like for HCl-doped PANI. Moreover, Figure 5-2 shows that all composites exhibit the same asymmetrical N(1s) spectrum as HCl-doped PANI. From

(28) Macdiarmid, A. G.; Epstein, A. J. *Faraday Discuss. Chem. Soc.* **1989**, *88*, 317.
(29) Asturias, G. E.; MacDiarmid, A. G.; McCall, R. P.; Epstein, A. J. *Synth. Met.* **1989**, *29*, 157.
(30) Snauwaert, P.; Lazzaroni, R.; Riga, J.; Verbist, J. J.; Gonbeau, D. *J. Chem. Phys.* **1990**, *92*, 2187.
(31) Kang, E. T.; Neoh, K. G.; Tan, T. C.; Khor, S. H.; Tan, K. L. *Macromolecules* **1990**, *23*, 2918.
(32) Kang, E. T.; Neoh, K. G.; Tan, K. L. *Synth. Met.* **1995**, *68*, 141.
(33) Zeng, X.-R.; Ko, T.-M. *Polymer* **1998**, *39*, 1187.
(34) Kang, E. T.; Neoh, K. G.; Tan, K. L. *Adv. Polym. Sci.* **1993**, *106*, 135.
(35) Kang, E. T.; Neoh, K. G.; Tan, K. L. *Prog. Polym. Sci.* **1998**, *23*, 277.
(36) Beamson, G.; Briggs, D. *High resolution XPS of organic polymer, the scienta ESCA300 database*; J. Wiley and Sons: New York, 1992.
(37) Snauwaert, P. Ph.D. Thesis, University of Namur, Namur, Belgium, 1992.

Table 1. XPS Surface Composition (atomic %) of Reference Polymers and PANI-Coated PS Latexes

series	sample	C	N	O	Cl	S
	NP40	76		24		
	PANI	74	10	13	0.5	2.5
1	PS(NP40)	97		3		
	PS(NP40)−PANI (80/20)	90	3.1	6	0.1	0.8
	PS(NP40)−PANI (65/35)	88	4.9	6	0.2	1
	PS(NP40)−PANI (47/53)	76	10	11.5	0.5	2
2	PS-CL(NP40)	97		3		
	PS-CL(NP40)−PANI (80/20)	87	2.5	10		0.9
3	PS-CL(NP40/Surfamid)	97		3.5		
	PS-CL(NP40/Surfamid)−PANI (80/20)	88	4.3	7	0.2	1

a quantitative point of view (see Table 1), the measured amount of nitrogen atoms at the surface increases from 3 to 10% from sample (b) to sample (d). These results allow us to conclude that PS latex is progressively covered by PANI when the PANI weight ratio increases.

Further information can be provided by the analysis of XPS valence spectra. Indeed, valence spectra scrutinize the electrons directly involved in the bonds between atoms, and consequently those that contain the best potential information. A detailed interpretation of an XPS valence spectrum requires the help of calculations, because it is representative of the density of states of the occupied energy levels close to the Fermi level. However, a valence spectrum can be more easily used as a fingerprint to identify a compound (or a mixing of a few compounds), which constitutes a completely different approach from the analysis of core peaks, and provides different information. For this reason, the valence spectra of all samples have been carefully recorded.

Figure 6 shows the valence spectra of the same samples. In this figure, we can see clearly that the valence spectra of PS−PANI composites gradually change from the valence spectrum of PS(NP40) to that of HCl-doped PANI as a function of the PANI weight ratio. Particularly, the valence spectrum of sample (d) (weight ratio 47/53) is very similar to that of PANI, which is in perfect agreement with the C(1s) core peak results (Figure 5). From a qualitative point of view, these results definitely show that the surface of the particle surface gets richer in PANI. However, PS still remains even at a high PANI concentration, which could be explained by a patchy coverage; see the following.

As mentioned before, different composites have been prepared from three different kinds of seed latexes with a fixed PS/PANI (80/20) weight ratio for comparison. Figure 7 shows the C(1s) and N(1s) spectra of (a) PS(NP40)−PANI (80/20), (b) PS-CL(NP40)−PANI (80/20), and (c) PS-CL(NP40/Surfamid)−PANI (80/20). We can notice in this figure that these spectra have similar shapes. N(1s) core peaks display the typical asymmetrical shape of PANI, while the C(1s) core peaks are very weakly broadened for this low PANI weight ratio. The difference observed in the C(1s) peak of sample (b) can be assigned to carbon atoms bound to one oxygen atom in the surfactant. The most important difference concerns the measured amount of nitrogen in these samples (see Table 1): 3.1% for sample (a), 2.5% for sample (b), and 4.3% for sample (c), showing that the PANI coverage depends on the synthesis method, as it will be detailed below.

Surface Composition and Conductivity Measurements. The PANI coverage at the surface of the seed latex can be estimated from the relative amounts of carbon and nitrogen atoms at the surface. Indeed, in HCl-doped PANI, the ratio between the amounts of nitrogen and carbon as measured by XPS is $(N/C)_{PANI} = 0.14$, which is very close to the theoretical value (0.167). Thus, from the $(N/C)_{PS-PANI}$ ratio measured in the different PS−PANI composites, the PANI coverage at the surface of the seed latex can be calculated according to eq 1, if we assume that the PANI thickness is greater than the XPS sampling depth, which means much greater than the photoelectron mean free path in PANI, which can be estimated at 3.6 nm according to a model appropriate for organic materials.[38]

$$\% \text{ PANI} = \frac{(N/C)_{PS-PANI}}{(N/C)_{PANI}} \quad (1)$$

The different PANI coverages calculated from the XPS analyses using this eq 1 have been reported in Table 2, as well as the results of the conductivity measurements. First, the results can be compared when the PANI content increases in the same series, PS(NP40)−PANI. As expected, the PANI coverage as well as the conductivity increase with the PANI weight ratio. It is worth noting that the very high PANI coverage (94%) calculated for sample PS(NP40)−PANI (47/53) is in good agreement with the shape observed for its C(1s) core peak and valence band spectra. Moreover, we can notice that an acceptable conductivity remains even at 26% of PANI coverage. These first results are better than the previous reports which described the XPS analysis of PS microparticles covered by PPy,[7,9,12] PANI,[6,13] or PEDOT.[8,11] These works showed that a uniform coverage was more difficult to obtain by using nanoscale core particles as well as PANI as the conductive polymer. The coverage of nanoscale PS was even less uniform, and SEM studies revealed a patchy PPy overlayer.[7,12] By optimizing the synthesis, the surface coverage increased up to 24% (PPy loading of 4.2 wt %), but the conductivity was lost ($<10^{-6}$ S/cm). No core coverage and conductivity results were done on a nanoscale PS core covered by PANI.

Then, the results of the three PS−PANI composites containing 20 wt % PANI can be compared. PS(NP40)−PANI and PS-CL(NP40)−PANI composites exhibit a similar surface coverage (26 and 21%, respectively). However, the conductivity is much greater (about five times) for the composite synthesized from the monodisperse PS seed latex. This feature can be related to a better PANI dispersion inside the PS matrix when processed. The important result is that the surface coverage increases up to 36% by using Surfamid as the surfactant, associated to a significant increase of the conductivity (0.7 S/cm). This latter result can be explained by the occurrence of H bond between the Surfamid amide group and the PANI backbone.[39] From these results, it can be concluded that the surfactant structure has a great impact on the properties of the final composite. Moreover, we show here that a high coverage is not required to obtain a conducting composite.

AFM Measurements. To better understand the particle formation and the shell shape, AFM analysis has been done on PS(NP40)−PANI, PS-CL(NP40)−PANI, and PS-CL(NP40/Surfamid)−PANI composites (Figure 8). PS(NP40)−PANI (Figure 8a) exhibits a disordered arrangement, and further comments are difficult. This feature may be due to the bimodal distribution of precursory PS(NP40) latex.

Then, samples were made from the monodisperse seed sample (Figure 1). However, discrete particles are no longer observed in the case of the composite, PS-CL(NP40/

(38) Seah, M. P.; Dench, W. A. *Surf. Interface Anal.* **1979**, *1*, 2.
(39) Ikkala, O. T.; Vikki, T.; Passiniemi, P.; Osterholm, H.; Osterholm, J.-E.; Pietila, L.-O.; Ahjopalo, L. *Synth. Met.* **1997**, *84*, 55.

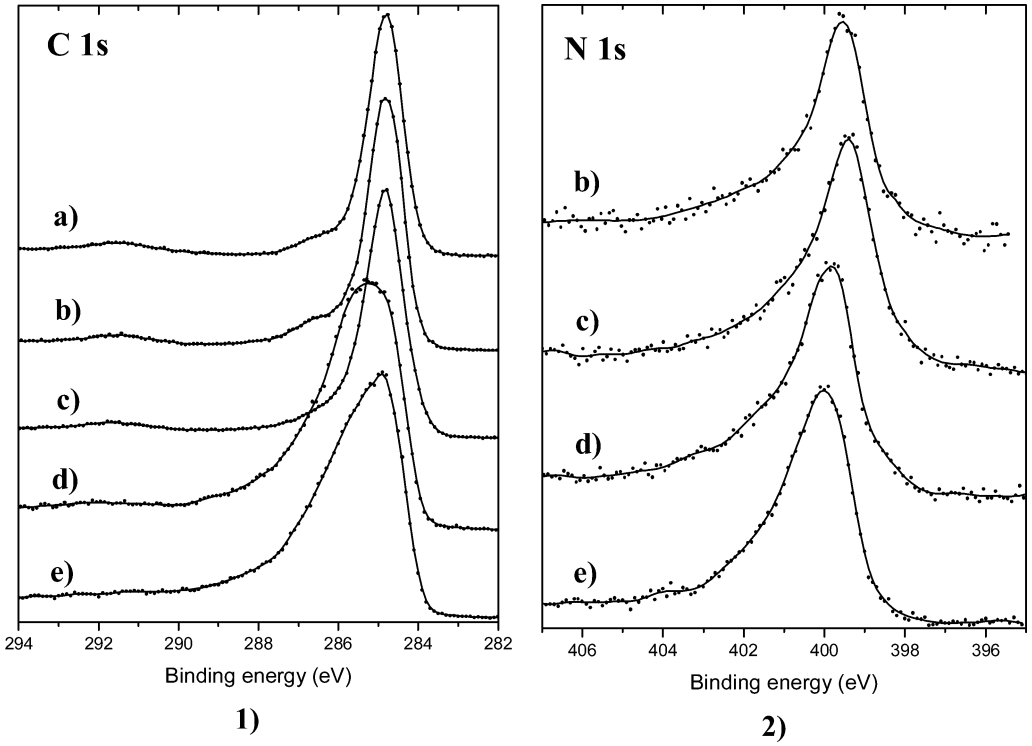

Figure 5. XPS (1) C(1s) and (2) N(1s) spectra of (a) PS(NP40), PS(NP40) coated with (b) 20, (c) 35, and (d) 50 wt % PANI, and (e) HCl-doped PANI.

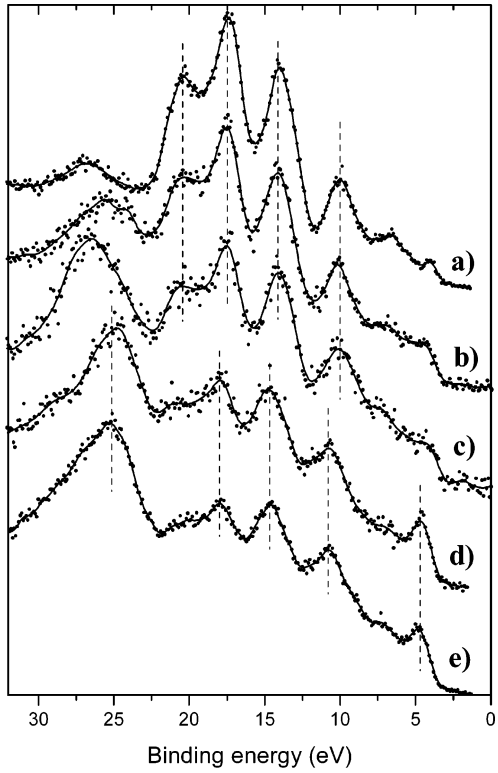

Figure 6. XPS valence spectra of (a) PS(NP40), PS(NP40) coated with (b) 20, (d) 35, and (c) 50 wt % PANI, and (e) HCl-doped PANI.

Surfamid)−PANI, Figure 8b. In this case, the determination of the coated particle size was very difficult. However, the composite sample consists of distinguishable grains. These images reveal the presence of a nonuniform PANI overlayer. The rms roughnesses measured (112 and 74 Å for Figure 8a,b, respectively) are definitely higher than the one measured for the fresh sample. Then, the patchy coverage of the seed PS latex is in agreement with those obtained by XPS.

SEM. The PS−PANI composites have been characterized by SEM analysis. The PS-CL(NP40) and corresponding composite containing 20 wt % PANI are presented in Figure 9. As expected, monodisperse PS latex particles have been observed by SEM (Figure 9a), which is in good agreement with AFM measurements (see Figure 1). However, the PANI overlayer clearly consists of patchy coating onto the PS particles (Figure 9b).

Discussion. At first, it is necessary to calculate the thickness of the PANI layer in a first hypothesis of the uniform layer and compare it to the photoelectron mean free path.

If we assume a uniform coverage (Figure 10) of the seed particles, the conducting polymer overlayer can be calculated by the following equation:[6]

$$d_{\mathrm{Ulayer}} = R\left[\sqrt[3]{\left(\frac{x_{\mathrm{mPANI}}\rho_{\mathrm{PS}}}{x_{\mathrm{mPS}}\rho_{\mathrm{PANI}}} + 1\right)} - 1\right] \qquad (2)$$

where d_{Ulayer} is the uniform PANI overlayer thickness, R is the radius of the PS core, x_{mPANI} is the PANI weight percent, ρ_{PANI} is the density of PANI ($\rho_{\mathrm{PANI}} = 1.4$ g·cm^{-3}),[6] x_{mPS} is the PS weight percent, and ρ_{PS} is the density of PS ($\rho_{\mathrm{PS}} = 1.05$ g·cm^{-3}).[6]

At 20 wt % PANI, the thickness of the overlayer of the PS-CL−PANI (80/20) is $d_{\mathrm{UPANI}} = 9$ nm, which is already above the photoelectron mean free path (estimated to 3.6 nm). However, XPS measurement did not exhibit a quantitative coverage of the core even at a higher PANI content because C(1s) peaks characteristic of PS are still present. This is in accordance with the image analysis, which showed a patchy overlayer.

To explain why a low PANI coverage can induce a good electrical conductivity, we propose here a very simple model of nonuniform coverage; see Figure 10. A spherical particle of PS with a radius R is partially covered by a

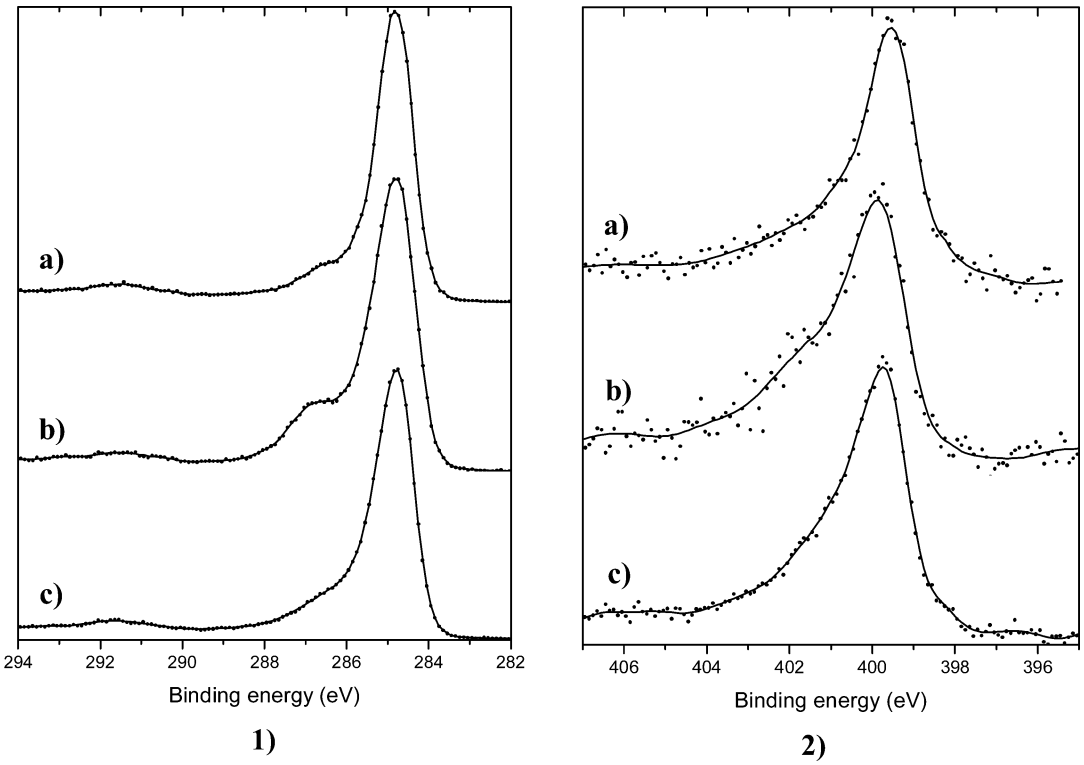

Figure 7. XPS (1) C(1s) and (2) N(1s) spectra of PS−PANI (80/20) composites with different PS latexes: (a) PS(NP40), (b) PS-CL(NP40), and (c) PS-CL(NP40/Surfamid).

Table 2. PANI Surface Coverage and Conductivity Measurements

sample	% PANI coverage	conductivity (S/cm)
PS(NP40)−PANI (80/20)	26	0.09 ± 0.01
PS(NP40)−PANI (65/35)	43	0.10 ± 0.01
PS(NP40)−PANI (47/53)	94	0.20 ± 0.02
PS-CL(NP40)−PANI (80/20)	21	0.50 ± 0.07
PS-CL(NP40/Surfamid)−PANI (80/20)	36	0.70 ± 0.10

noncontinuous spherical PANI shell with a thickness d_{NUlayer} (Figure 10). For a monodisperse and unimodal distribution of PS particles, the volume of PANI deposited on the PS core is given by the following equation:

$$d_{\mathrm{NUlayer}} = R\left[\sqrt[3]{\left(\frac{x_{\mathrm{mPANI}}}{1-x_{\mathrm{mPANI}}}\frac{\rho_{\mathrm{PS}}}{\rho_{\mathrm{PANI}}}\frac{1}{\alpha}+1\right)}-1\right] \quad (3)$$

where α represents the PANI coverage percent.

Equation 3 gives the following PANI thicknesses: $d_{\mathrm{NUlayer}} = 43$ nm for PS-CL(NP40)−PANI (80/20) and 26 nm for PS-CL(NP40/Surfamid)−PANI (80/20). It is worth noting that for the same PANI content, the coverage of the latex seed is much more uniform when Surfamid is used.

Other authors showed that the adsorption of PANI at a surface depends on many parameters.[40] The PANI coverage can be affected if the surface contains groups that interact with the conducting polymer and facilitate its adsorption to create a more uniform layer (lower value of d_{NUlayer}). This is well achieved by the Surfamid in our system, as expected.

For a bimodal distribution of two monodisperse PS particle populations (two particles radii R_1 and R_2), if we assume that the PANI thickness and the coverage are constant whatever the radius of the PS particle, the volume of PANI deposited on the PS core is given by the following equation:

$$V_{\mathrm{PANI}} = \frac{4}{3}\pi\alpha\left\{x_1{R_1}^3\left[\left(1+\frac{d_{\mathrm{NUlayer}}}{R_1}\right)^3-1\right]+ x_2{R_2}^3\left[\left(1+\frac{d_{\mathrm{NUlayer}}}{R_2}\right)^3-1\right]\right\} \quad (4)$$

where α represents the PANI coverage percent, d_{NUlayer} is the PANI thickness, R_1 and R_2 are the radii of both kinds of PS particles, and x_1 and x_2 are the percents of both kinds of PS particles.

Then, the PANI thickness is given by resolution of the following equation:

$$\frac{V_{\mathrm{PANI}}}{V_{\mathrm{PS}}} = \alpha\left\{x_1{R_1}^3\left[\left(1+\frac{d_{\mathrm{NUlayer}}}{R_1}\right)^3-1\right]+ x_2{R_2}^3\left[\left(1+\frac{d_{\mathrm{NUlayer}}}{R_2}\right)^3-1\right]\right\}/(x_1{R_1}^3+x_2{R_2}^3) = \frac{x_{\mathrm{mPANI}}}{\rho_{\mathrm{PANI}}}\frac{\rho_{\mathrm{PS}}}{1-x_{\mathrm{mPANI}}} \quad (5)$$

For the series of samples that exhibit a bimodal distribution of two monodisperse particle populations, namely, PS(NP40)−PANI (62% with $R_1 = 180$ nm, 38% with $R_2 = 70$ nm), eq 5 gives the following PANI coverage thicknesses for the following PS/PANI weight ratios 80/20, 65/35, and 47/53 as respectively 34, 42, and 40 nm.

All these values are much greater than the photoelectron mean free path (3.6 nm), so no correction has to be applied to the calculation of the PANI coverage α and the values reported in Table 2 are reliable. This confirms that the

(40) Pud, A.; Ogurtsov, N.; Korzhenko, A.; Shapoval, G. *Prog. Polym. Sci.* **2003**, *28*, 1701.

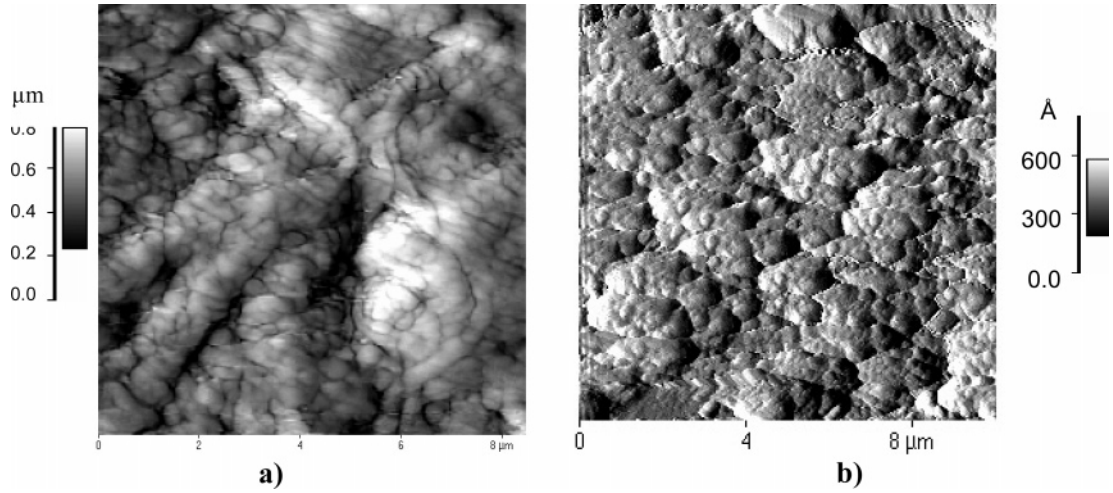

Figure 8. AFM images of composite (a) PS(NP40)−PANI and (b) PS-CL(NP40)−PANI (80/20).

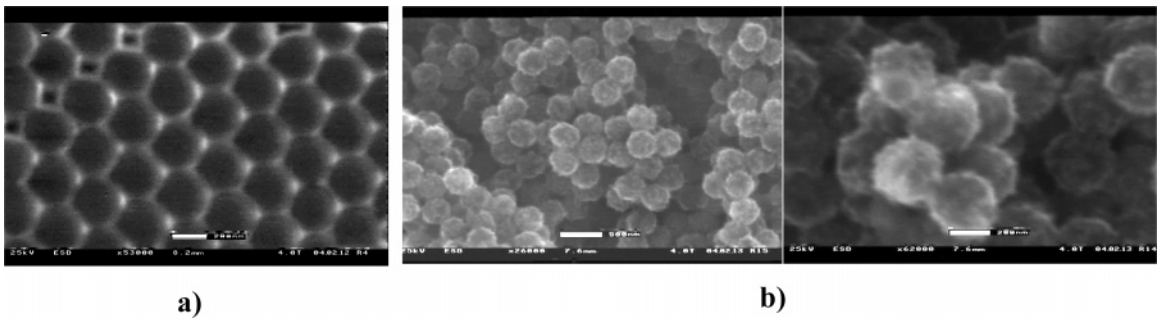

Figure 9. SEM images of (a) PS-CL(NP40) latex particles and (b) PS-CL(NP40)−PANI (80/20) core−shell particles.

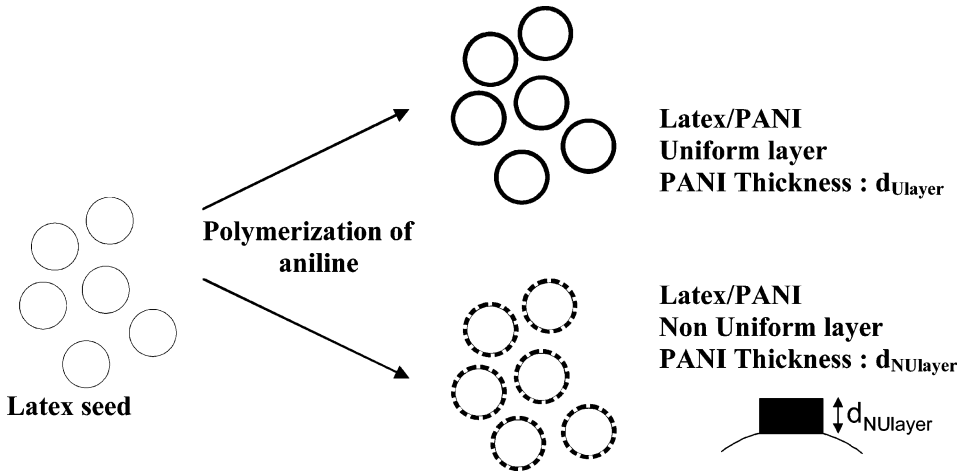

Figure 10. Schematic representation of uniform and nonuniform coverage.

coverage is actually patchy. However, it is worth noting that the PANI thickness d_{NUlayer} remains almost unchanged for a wide range of compositions in a same series of PS−PANI composites. This observation suggests that PANI is deposited at the surface of the PS particles with a minimum thickness and that the increase of the PANI weight percent mainly results in the increase of the coverage without substantial increase of the thickness, the coverage α being proportional to the number of PANI nanoparticles.

However, the fact that a low PANI coverage can result in a good electric conductivity remains to be explained.

From this geometrical model and the experimental results, a schematic representation of the aggregation can be done. The discrete PANI overlayer is assimilated to half-spherical deposits where the radius is d_{NUlayer}. This takes in account the image analysis, the XPS results, and the conductivity measurements. A model is sketched in Figure 11.

The core particles are covered by discrete nanodeposits of PANI in agreement with the XPS and SEM results. There are enough conductive deposits on each PS seed particle to create a continuous conducting network when the samples are processed. The percolation threshold is reached when the distance between the conductive disks is smaller than the diameter of the disks (i.e., $2d_{\mathrm{NUlayer}}$). This feature explains the good conductivity reported at low PANI content.

The PS-CL(NP40)−PANI (80/20) coverage was estimated to 21% by XPS measurement (Table 2). The overlayer thickness of 43 nm (d_{NUlayer} from eq 2) corresponds to an average of 14 half-spherical PANI deposits

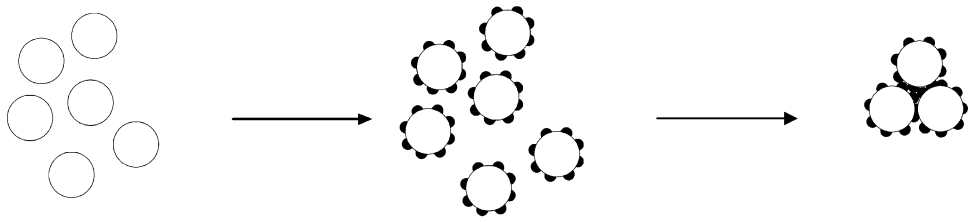

Figure 11. Schematic representation of (a) seed PS particles, (b) PS−PANI composite particles with PANI nanoparticles onto the surface of PS latex, and (c) the conducting network formation.

per core particle. If we assume that these deposits are organized in a hexagonal structure, the distance between each deposit is 80 nm, which is slightly below the diameter of the PANI disk (86 nm). A conducting continuum is created when processed (as sketched in Figure 11). The same calculation can be done for the PS-CL(NP40/Surfamid)−PANI. The PANI overlayer of the PS-CL-(NP40/Surfamid)−PANI (80/20) is constituted by 61 half-spherical deposits (radius, $d_{\mathrm{NUlayer}} = 26$ nm). The distance between each deposit is 25 nm, which is far below the theoretical percolation threshold.

It is worth noting that this model predicts a theoretical percolation threshold around 20 wt % PANI for the composite PS-CL(NP40)−PANI. However, the 10 wt % PANI composite still exhibits an acceptable conductivity (0.1 S/cm). In the above percolation model, the PANI deposits as well as the PS core do not lose their shape, and this statement can overestimate the percolation threshold. It is likely that the PANI deposits are crushed on the core particles during the process. This would lower the percolation threshold results.

Another important point that should be clarified is the origin of the patchy deposit of PANI at the latex seed surface. Other authors[41] studied the synthesis of PS latexes. A steric stabilizer was used, and the chemical composition at the particle surface was studied by XPS analysis. They showed that the surfactant overlayer was not uniform and thick agglomerates incompletely cover the PS particles. One must keep in mind that the nature of the coverage, uniform or patchy, should be monitored by interactions between PANI and chemical groups available at the interface.

(41) Deslandes, Y.; Mitchell, D. F.; Paine, A. J. *Langmuir* **1993**, *9*, 1468.

Conclusion

Three kinds of PANI-coated PS latexes have been prepared and characterized by XPS, AFM, SEM, and conductivity measurements. These techniques confirmed that PS seed latexes synthesized with a cross-linked agent have a monodisperse size distribution and that particles are organized in a hexagonal structure. Close inspection of the surface composition and C(1s) spectra of the coated latexes confirmed that the PS particle surface is covered by discrete deposits of PANI. XPS measurements showed a maximum coverage of 94%. Using a surfactant bearing an amide group reinforces the surface coverage and consequently the conductivity. The analysis showed that a quantitative coverage of the seed particles is not necessary to obtain a good conductivity value. However, a monodisperse PS latex, an appropriate surfactant, and a sufficient amount of PANI are the criteria to create a conducting network when processing.

Acknowledgment. The authors would like to express their gratitude to Dr. Christelle Guerret and Dr. François Roby (LPCP, UMR 5067) for helpful discussions. They also thank Mr. Abdel Khoukh (LPCP, UMR 5067) for NMR analysis.

LA0481243